CHAPTER e14

Atlas of Urinary Sediments and Renal Biopsies

Agnes B. Fogo
Eric G. Neilson

Key diagnostic features of selected diseases in renal biopsy are illustrated, with light, immunofluorescence, and electron microscopic images. Common urinalysis findings are also documented.

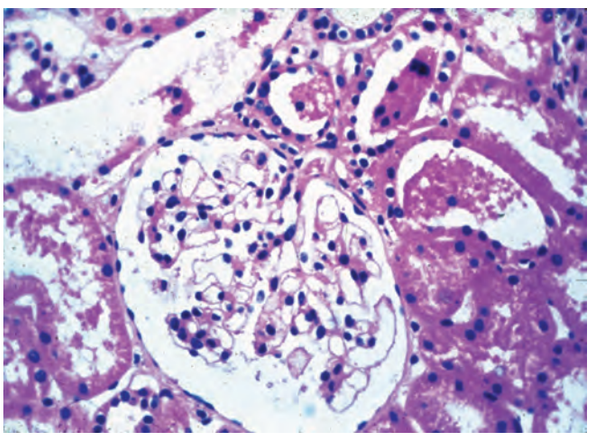

A

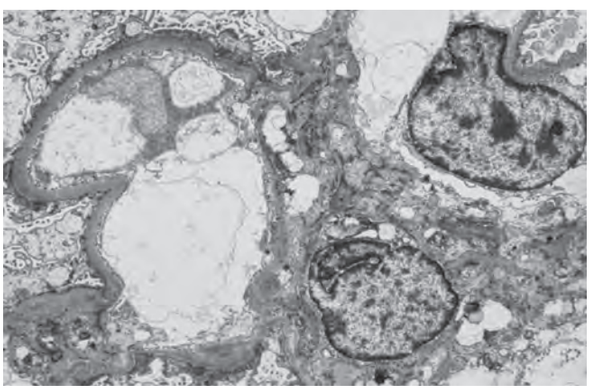

B

Figure e14-1 Minimal-change disease. In minimal-change disease, light microscopy is unremarkable **(A)**, while electron microscopy **(B)** reveals podocyte injury evidenced by complete foot process effacement. *(ABF/Vanderbilt Collection.)*

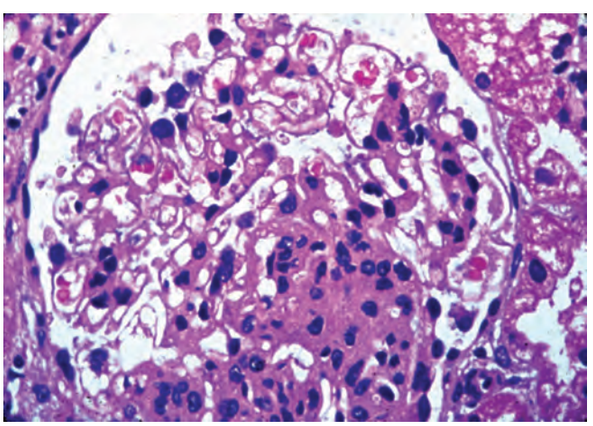

Figure e14-2 Focal segmental glomerulosclerosis (FSGS). There is a well-defined segmental increase in matrix and obliteration of capillary loops, the sine qua non of segmental sclerosis not otherwise specified (nos) type. *(EGN/UPenn Collection.)*

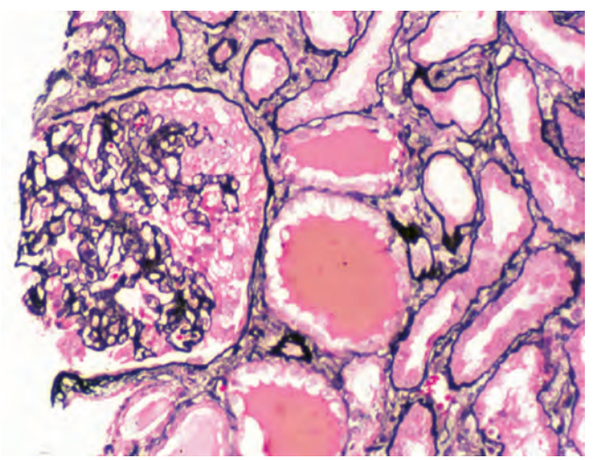

Figure e14-3 Collapsing glomerulopathy. There is segmental collapse of the glomerular capillary loops and overlying podocyte hyperplasia. This lesion may be idiopathic or associated with HIV infection and has a particularly poor prognosis. *(ABF/Vanderbilt Collection.)*

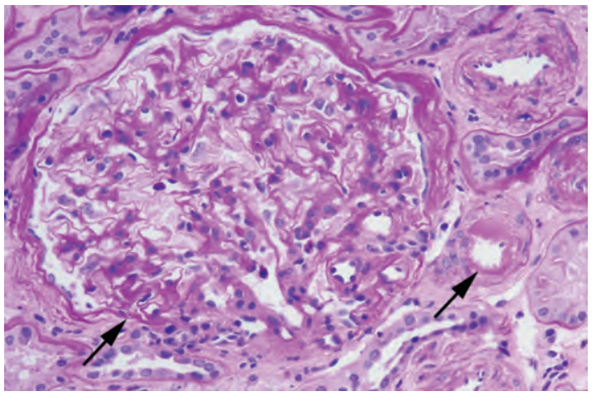

Figure e14-4 **Hilar variant of FSGS.** There is segmental sclerosis of the glomerular tuft at the vascular pole with associated hyalinosis, also present in the afferent arteriole (*arrows*). This lesion often occurs as a secondary response when nephron mass is lost due to, e.g., scarring from other conditions. Patients usually have less proteinuria and less steroid response than FSGS, nos type. *(ABF/Vanderbilt Collection.)*

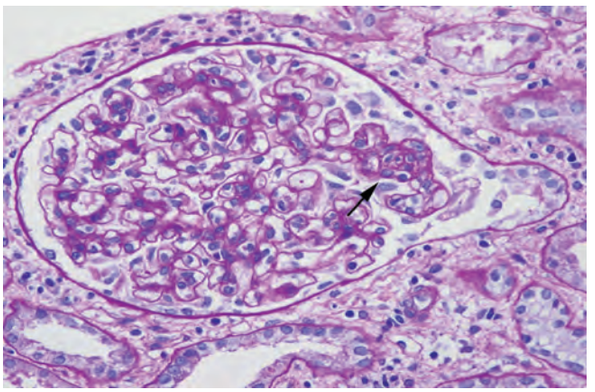

Figure e14-5 **Tip lesion variant of FSGS.** There is segmental sclerosis of the glomerular capillary loops at the proximal tubular outlet (*arrow*). This lesion has a better prognosis than other types of FSGS. *(ABF/Vanderbilt Collection.)*

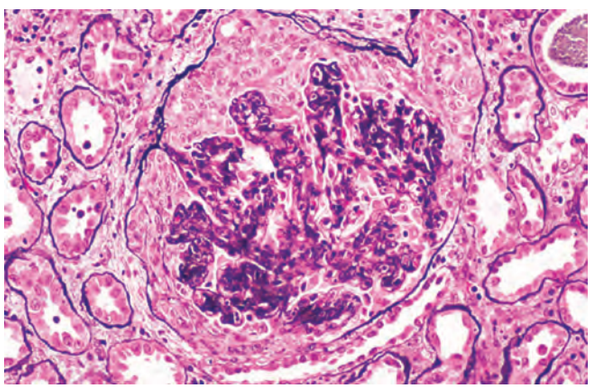

A

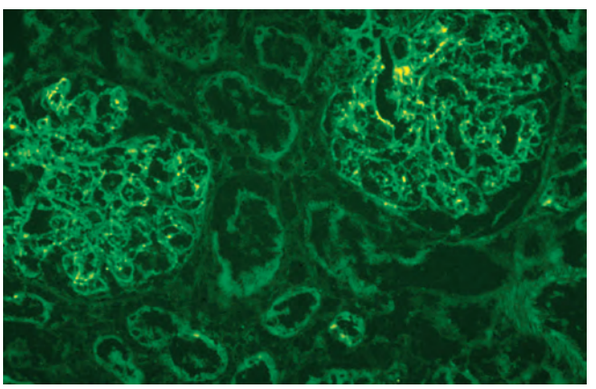

B

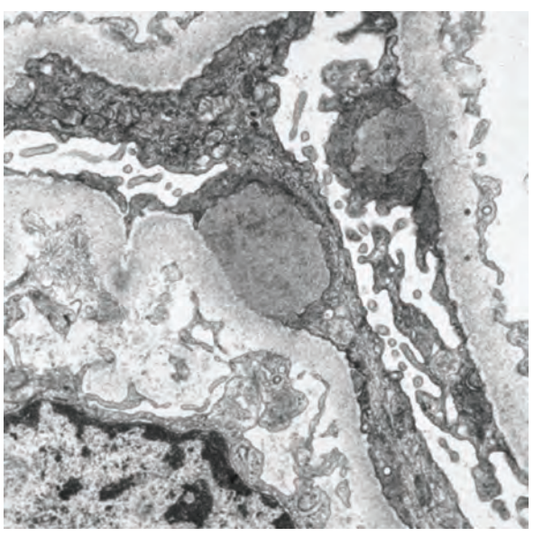

C

Figure e14-6 **Postinfectious (poststreptococcal) glomerulonephritis.** The glomerular tuft shows proliferative changes with numerous PMNs, with a crescentic reaction in severe cases (**A**). These deposits localize in the mesangium and along the capillary wall in a subepithelial pattern and stain dominantly for C3 and to a lesser extent for IgG (**B**). Subepithelial hump-shaped deposits are seen by electron microscopy (**C**). *(ABF/Vanderbilt Collection.)*

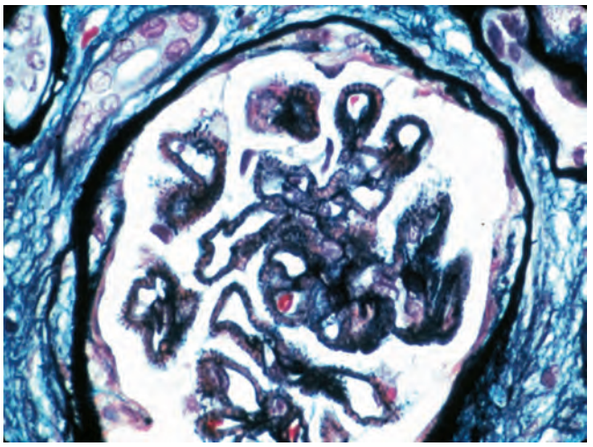

A

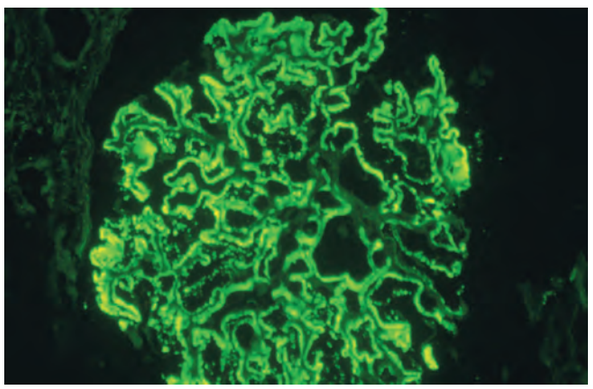

B

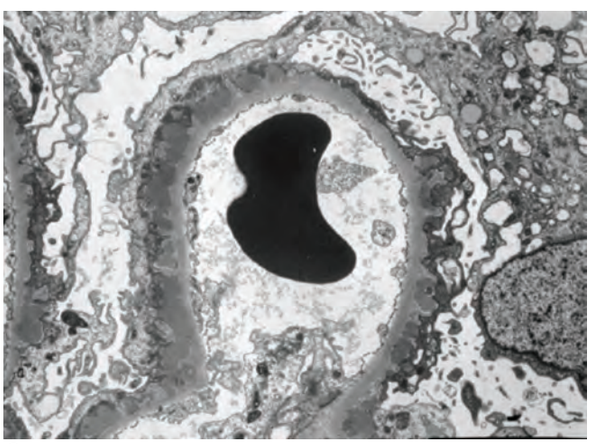

C

Figure e14-7 Membranous glomerulopathy. Membranous glomerulopathy is due to subepithelial deposits, with resulting basement membrane reaction, resulting in the appearance of spike-like projections on silver stain (**A**). The deposits are directly visualized by fluorescent anti-IgG, revealing diffuse granular capillary loop staining (**B**). By electron microscopy, the subepithelial location of the deposits and early surrounding basement membrane reaction is evident, with overlying foot process effacement (**C**). *(ABF/Vanderbilt Collection.)*

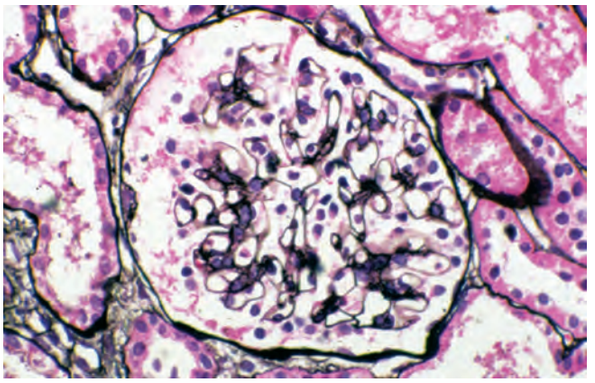

A

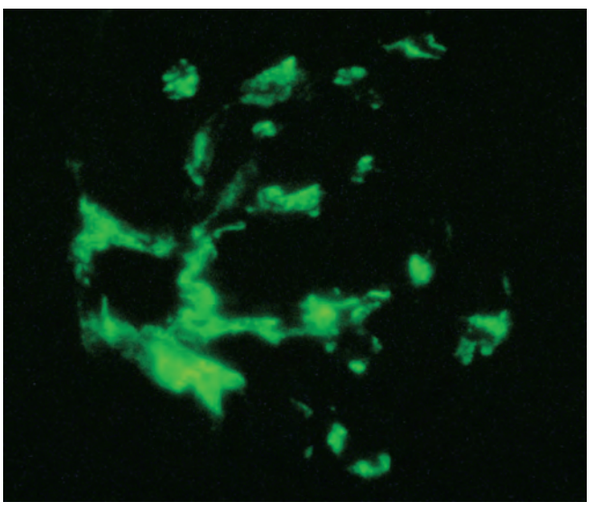

B

Figure e14-8 IgA nephropathy. There is variable mesangial expansion due to mesangial deposits, with some cases also showing endocapillary proliferation or segmental sclerosis (**A**). By immunofluorescence, mesangial IgA deposits are evident (**B**). *(ABF/Vanderbilt Collection.)*

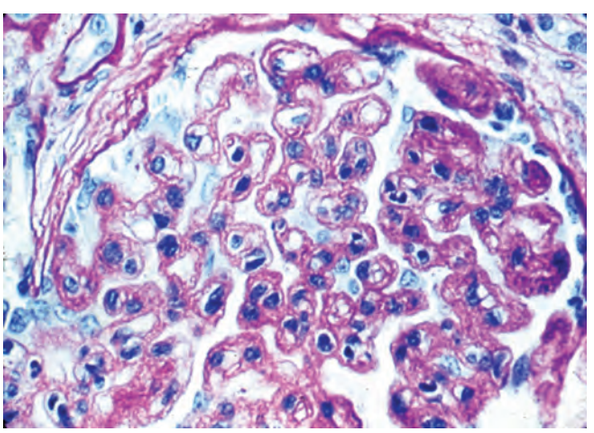

Figure e14-9 Membranoproliferative glomerulonephritis. There is mesangial expansion and endocapillary proliferation with cellular interposition in response to subendothelial deposits, resulting in the "tram-track" of duplication of glomerular basement membrane. *(EGN/UPenn Collection.)*

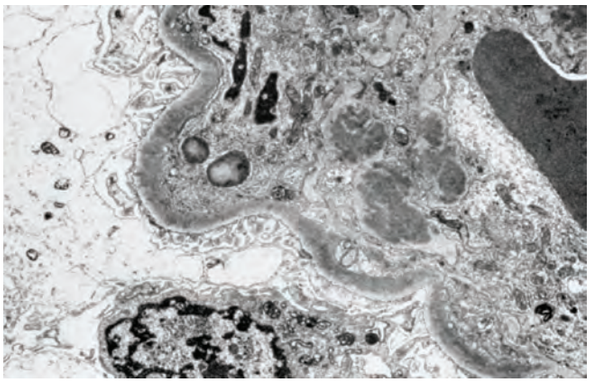

Figure e14-10 Dense deposit disease (membranoproliferative glomerulonephritis type II). By light microscopy, there is a membranoproliferative pattern. By electron microscopy, there is a dense transformation of the glomerular basement membrane with round, globular deposits within the mesangium. By immunofluorescence, only C3 staining is usually present. *(ABF/Vanderbilt Collection.)*

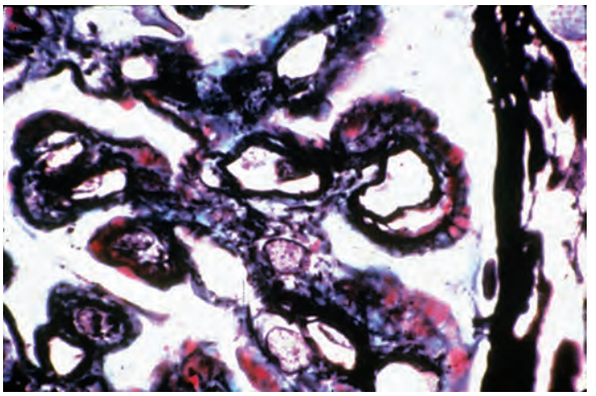

Figure e14-11 Mixed proliferative and membranous glomerulonephritis. This specimen shows pink subepithelial deposits with spike reaction, and the "tram-track" sign of reduplication of glomerular basement membrane, resulting from subendothelial deposits, as may be seen in mixed membranous and proliferative lupus nephritis (ISN/RPS class V and IV). *(EGN/UPenn Collection.)*

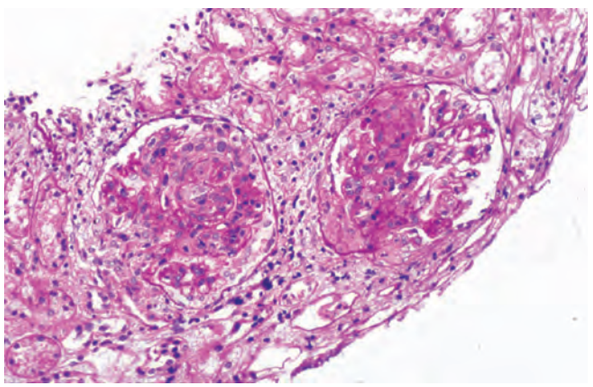

A

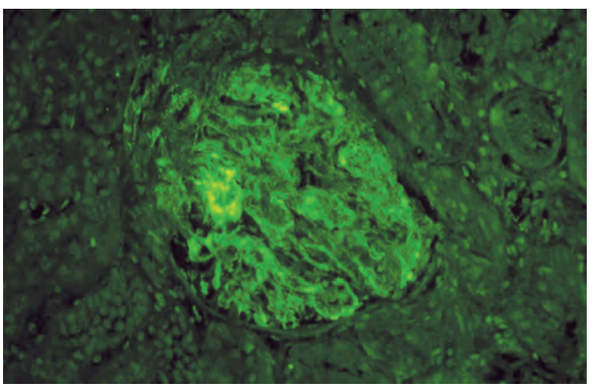

B

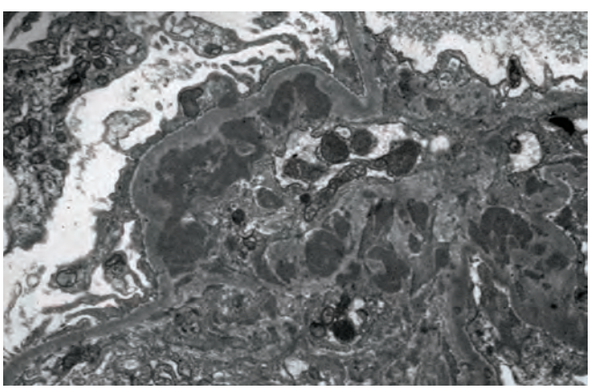

C

Figure e14-12 Lupus nephritis. Proliferative lupus nephritis, ISN/RPS class III (focal) or IV (diffuse), manifests as endocapillary proliferation, which may result in segmental necrosis due to deposits, particularly in the subendothelial area (**A**). By immunofluorescence, chunky irregular mesangial and capillary loop deposits are evident, with some of the peripheral loop deposits having a smooth, molded outer contour due to their subendothelial location. These deposits typically stain for all three immunoglobulins, IgG, IgA, IgM, and both C3 and C1q (**B**). By electron microscopy, subendothelial, mesangial, and rare subepithelial dense immune complex deposits are evident, along with extensive foot process effacement (**C**). *(ABF/Vanderbilt Collection.)*

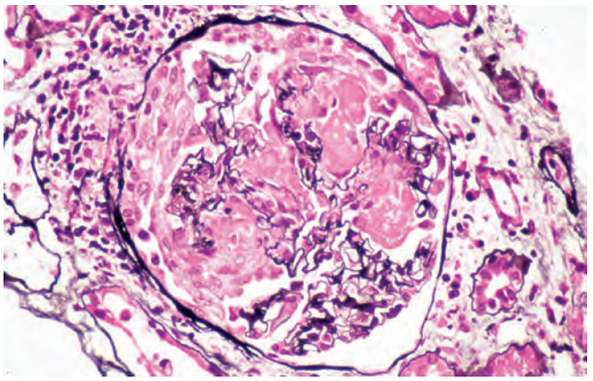

Figure e14-13 Granulomatosis with polyangiitis (Wegener's). This pauci-immune necrotizing crescentic glomerulonephritis shows numerous breaks in the glomerular basement membrane with associated segmental fibrinoid necrosis, and a crescent formed by proliferation of the parietal epithelium. Note that the uninvolved segment of the glomerulus (at ~5 o'clock) shows no evidence of proliferation or immune complexes. *(ABF/Vanderbilt Collection.)*

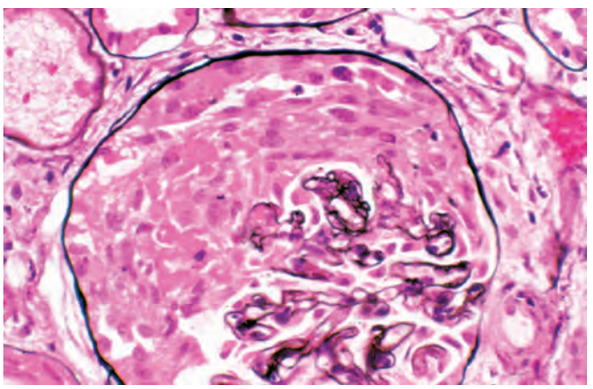

A

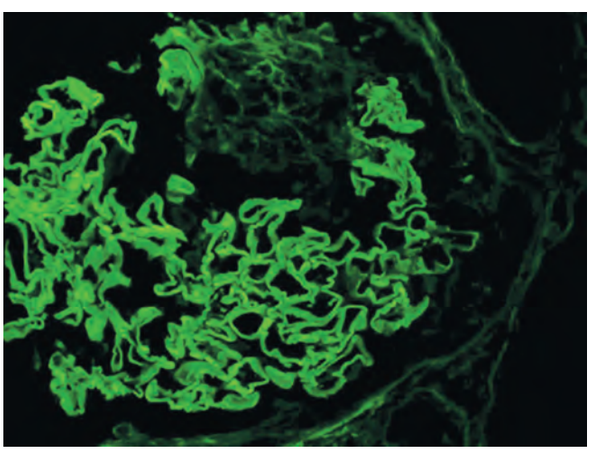

B

Figure e14-14 Anti-GBM antibody-mediated glomerulonephritis. There is segmental necrosis with a break of the glomerular basement membrane and a cellular crescent (**A**), and immunofluorescence for IgG shows linear staining of the glomerular basement membrane with a small crescent at ~1 o'clock (**B**). *(ABF/Vanderbilt Collection.)*

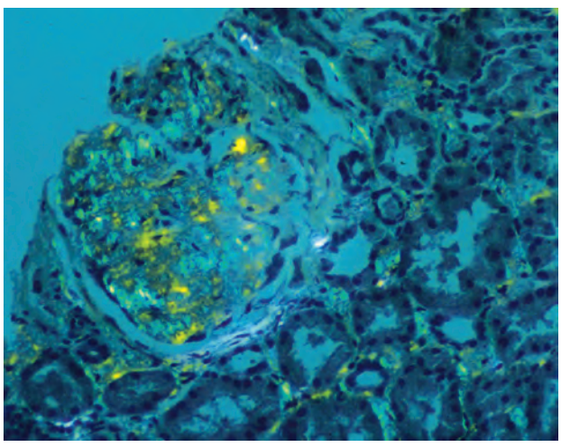

A

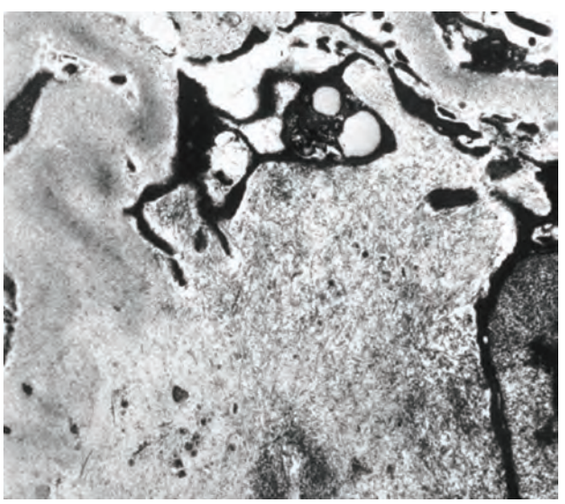

B

Figure e14-15 Amyloidosis. Amyloidosis shows amorphous, acellular expansion of the mesangium, with material often also infiltrating glomerular basement membranes, vessels, and in the interstitium, with apple-green birefringence by polarized congo red stain (**A**). the deposits are composed of randomly organized 9- to 11-nm fibrils by electron microscopy (**B**). *(ABF/Vanderbilt collection.)*

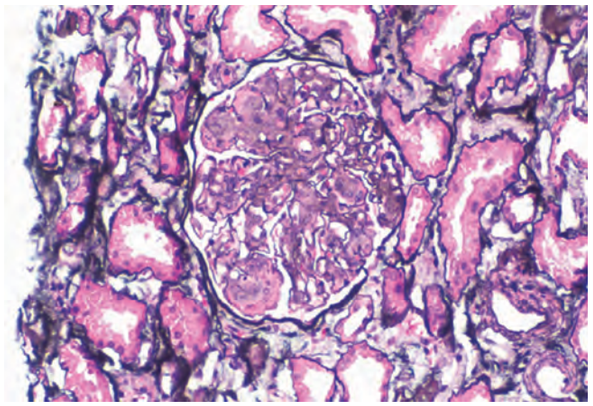

A

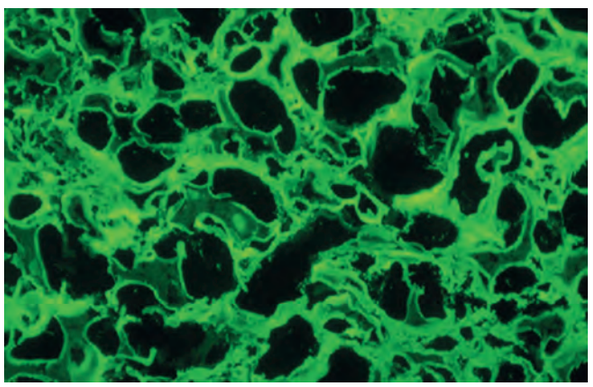

B

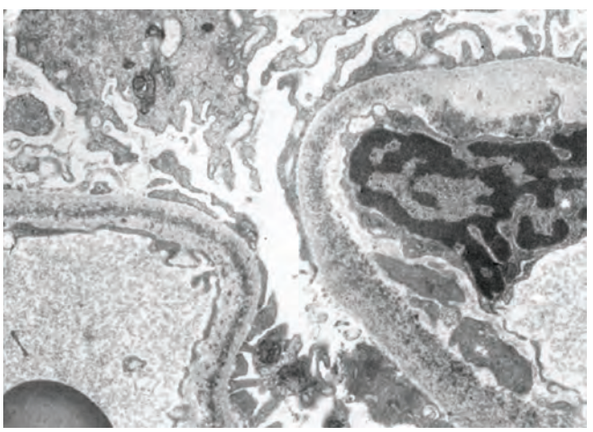

C

Figure e14-16 **Light chain deposition disease.** There is mesangial expansion, often nodular by light microscopy (**A**), with immunofluorescence showing monoclonal staining, more commonly with kappa than lambda light chain, of tubules (**B**) and glomerular tufts. By electron microscopy (**C**), the deposits show an amorphous granular appearance and line the inside of the glomerular basement membrane and are also found along the tubular basement membranes. *(ABF/Vanderbilt Collection.)*

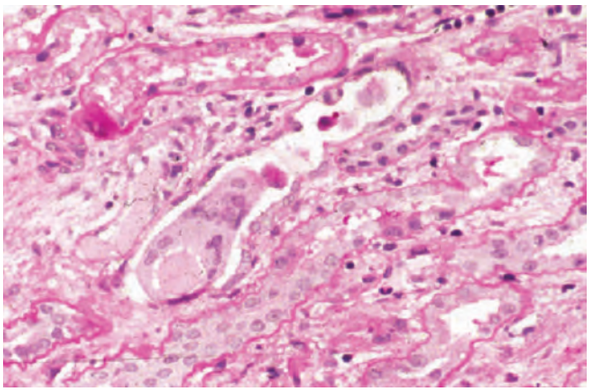

Figure e14-17 **Light chain cast nephropathy (myeloma kidney).** Monoclonal light chains precipitate in tubules and result in a syncytial giant cell reaction surrounding the casts, and a surrounding chronic interstitial nephritis with tubulointerstitial fibrosis. *(ABF/Vanderbilt Collection.)*

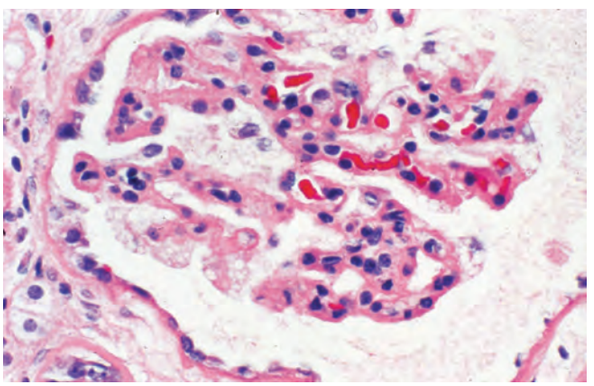

A

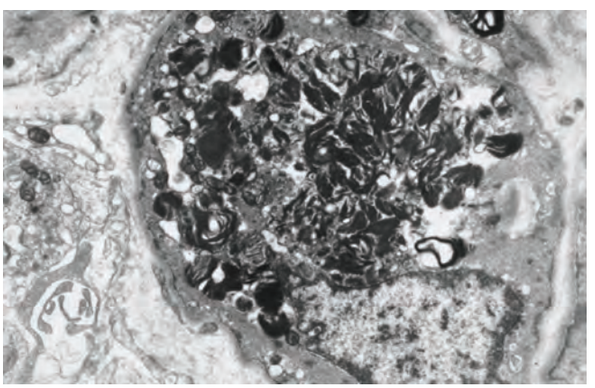

B

Figure e14-18 **Fabry's disease.** Due to deficiency of α-galactosidase, there is abnormal accumulation of glycolipids, resulting in foamy podocytes by light microscopy (**A**). These deposits can be directly visualized by electron microscopy (**B**), where the glycosphingolipid appears as whorled so-called myeloid bodies, particularly in the podocytes. *(ABF/Vanderbilt Collection.)*

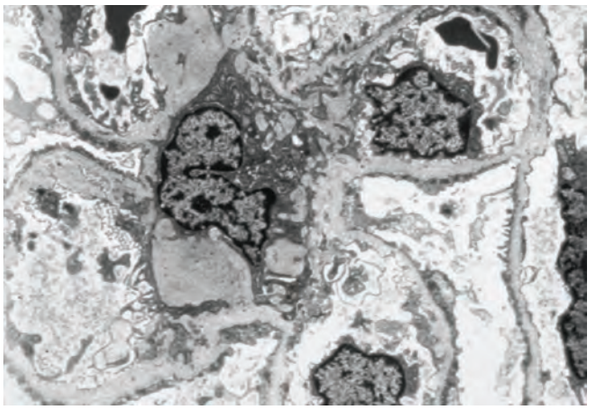

A

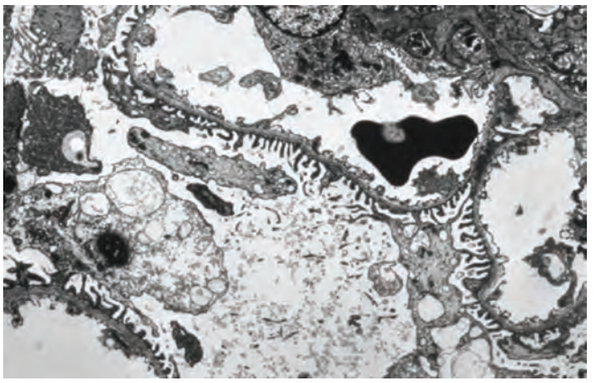

B

Figure e14-19 Alport's syndrome and thin glomerular basement membrane lesion. In Alport's syndrome, there is irregular thinning alternating with thickened so-called basket-weaving abnormal organization of the glomerular basement membrane (**A**). In benign familial hematuria, or in early cases of Alport's syndrome or female carriers, only extensive thinning of the GBM is seen by electron microscopy (**B**). *(ABF/Vanderbilt Collection.)*

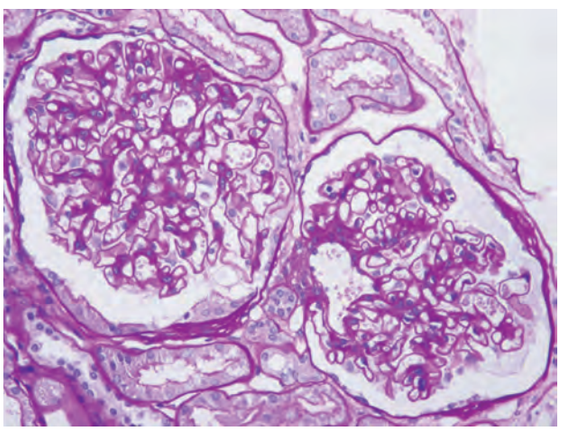

A

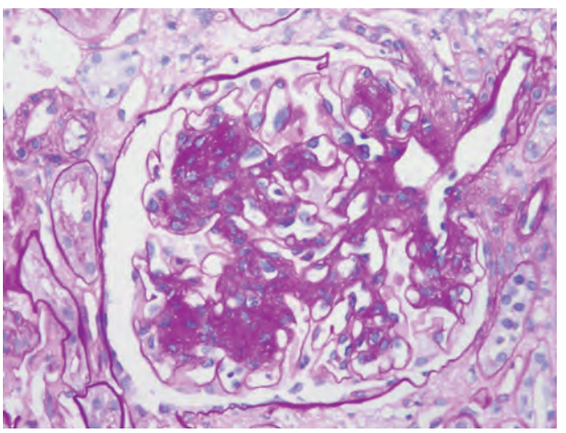

B

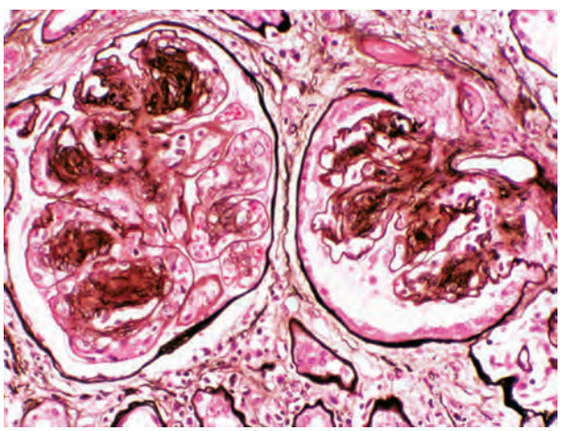

C

Figure e14-20 Diabetic nephropathy. In the earliest stage of diabetic nephropathy, only mild mesangial increase and prominent glomerular basement membranes (confirmed to be thickened by electron microscopy) are present (**A**). In slightly more advanced stages, more marked mesangial expansion with early nodule formation develops, with evident arteriolar hyaline (**B**). In established diabetic nephropathy, there is nodular mesangial expansion, so-called Kimmelstiel-Wilson nodules, with increased mesangial matrix and cellularity, microaneurysm formation in the glomerulus on the left, and prominent glomerular basement membranes without evidence of immune deposits and arteriolar hyalinosis of both afferent and efferent arterioles (**C**). *(ABF/Vanderbilt Collection.)*

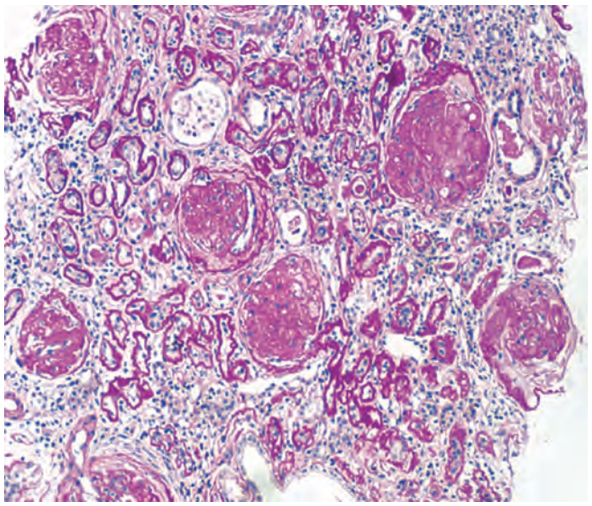

A

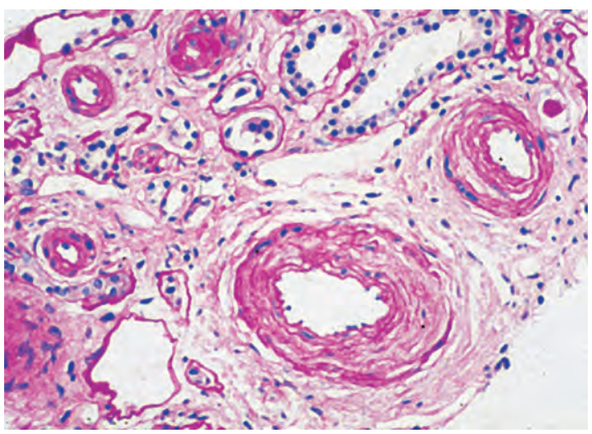

B

Figure e14-21 **Arterionephrosclerosis.** Hypertension-associated injury often manifests extensive global sclerosis of glomeruli, with accompanying and proportional tubulointerstitial fibrosis and pericapsular fibrosis, and there may be segmental sclerosis (**A**). The vessels show disproportionately severe changes of intimal fibrosis, medial hypertrophy, and arteriolar hyaline deposits (**B**). *(ABF/Vanderbilt Collection.)*

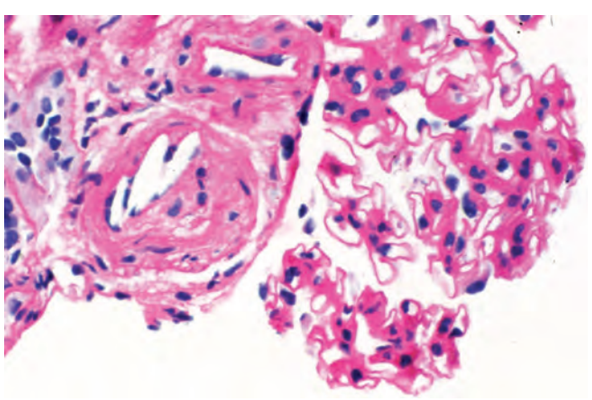

Figure e14-22 **Cholesterol emboli.** Cholesterol emboli cause cleft-like spaces where the lipid has been extracted during processing, with smooth outer contours, and surrounding fibrotic and mononuclear cell reaction in these arterioles. *(ABF/Vanderbilt Collection.)*

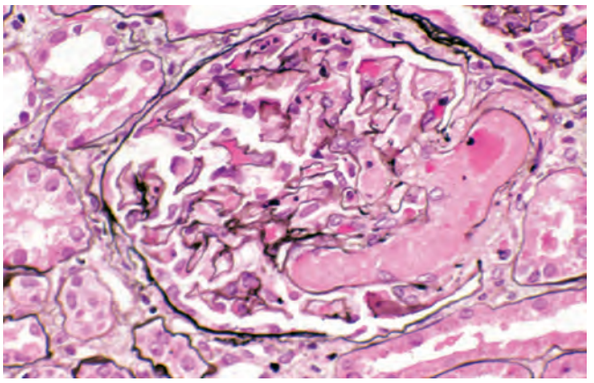

Figure e14-23 **Hemolytic uremic syndrome.** There are characteristic intraglomerular fibrin thrombi, with a chunky pink appearance (thrombotic microangiopathy). The remaining portion of the capillary tuft shows corrugation of the glomerular basement membrane due to ischemia. *(ABF/Vanderbilt Collection.)*

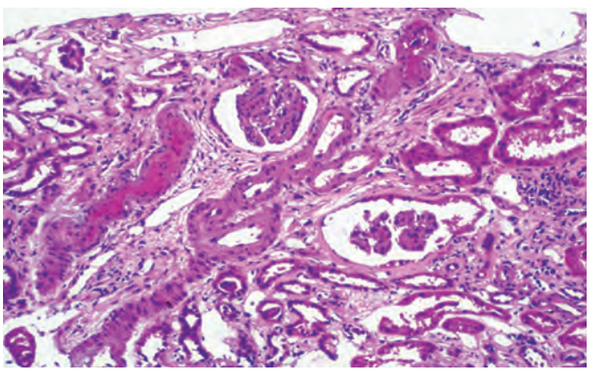

A

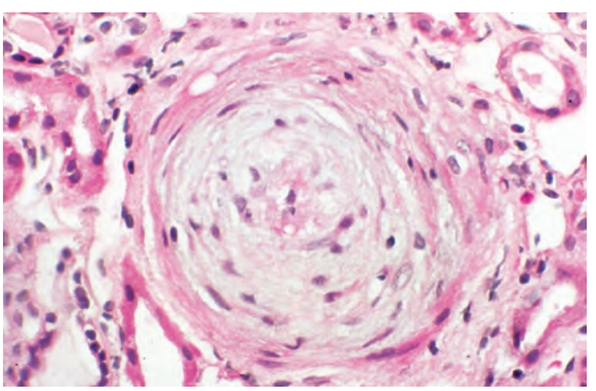

B

Figure e14-24 **Progressive systemic sclerosis.** Acutely, there is fibrinoid necrosis of interlobular and larger vessels, with intervening normal vessels and ischemic change in the glomeruli (**A**). Chronically, this injury leads to intimal proliferation, the so-called onion-skinning appearance (**B**). *(ABF/Vanderbilt Collection.)*

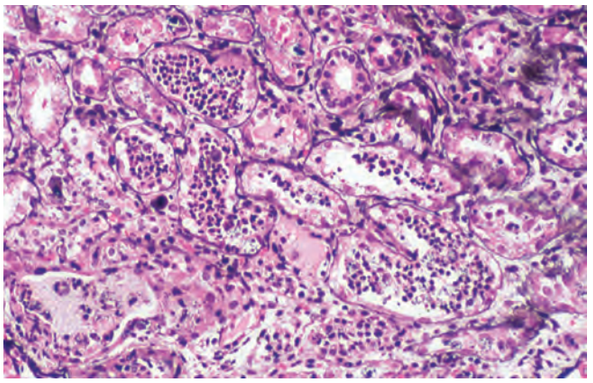

Figure e14-25 **Acute pyelonephritis.** There are characteristic intratubular plugs and casts of PMNs with inflammation extending into the surrounding interstitium, and accompanying tubular injury. *(ABF/Vanderbilt Collection.)*

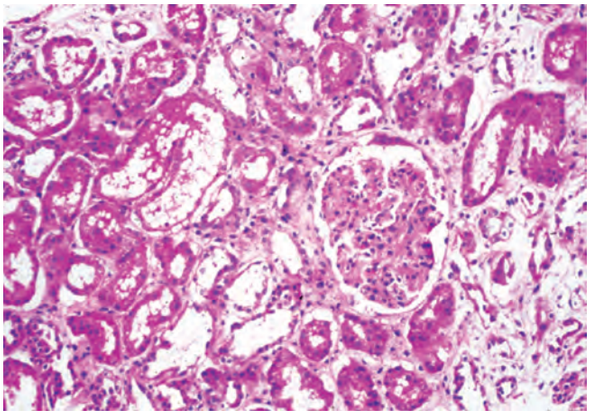

Figure e14-26 **Acute tubular injury.** There is extensive flattening of the tubular epithelium and loss of the brush border, with mild interstitial edema, characteristic of acute tubular injury due to ischemia. *(ABF/Vanderbilt Collection.)*

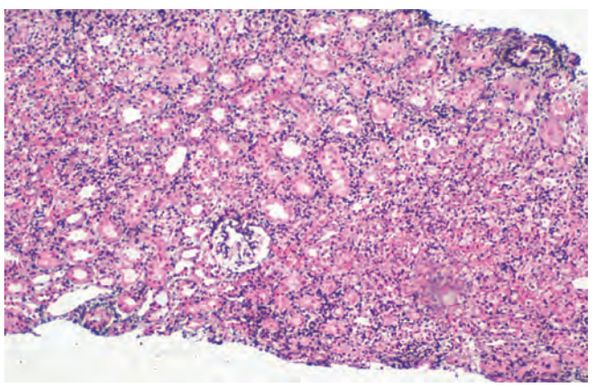

A

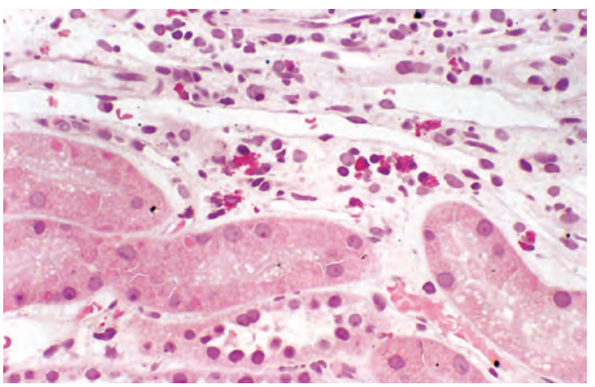

B

Figure e14-27 **Acute interstitial nephritis.** There is extensive interstitial lymphoplasmocytic infiltrate with mild edema and associated tubular injury (**A**), which is frequently associated with interstitial eosinophils (**B**) when caused by a drug hypersensitivity reaction. *(ABF/Vanderbilt Collection.)*

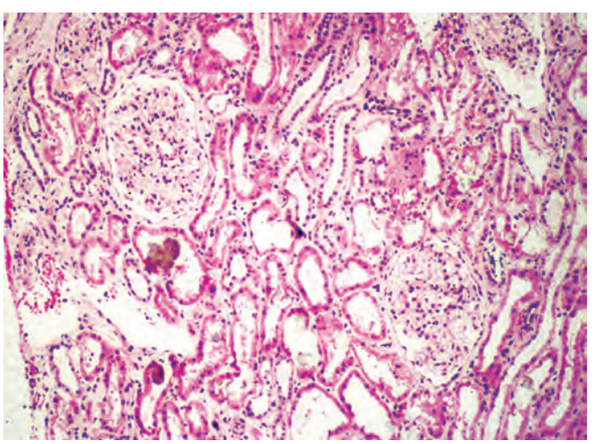

A

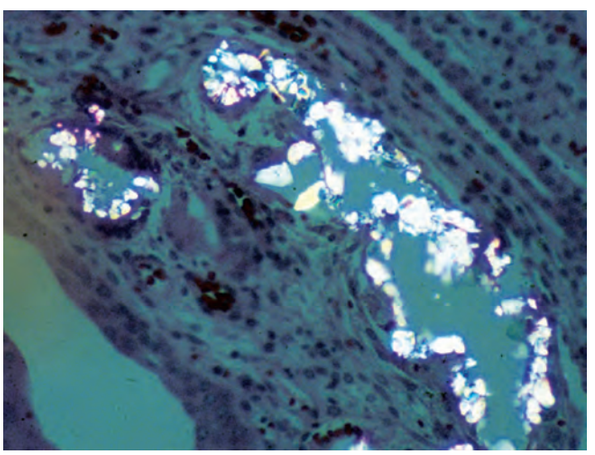

B

Figure e14-28 **Oxalosis**. Calcium oxalate crystals have caused extensive tubular injury, with flattening and regeneration of tubular epithelium (**A**). Crystals are well visualized as sheaves when viewed under polarized light (**B**). *(ABF/Vanderbilt Collection.)*

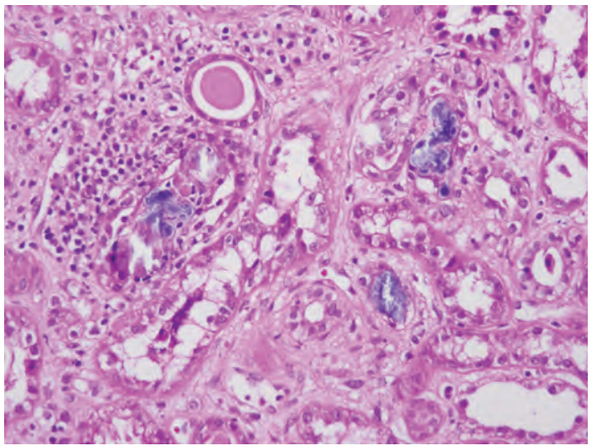

Figure e14-29 **Acute phosphate nephropathy.** There is extensive acute tubular injury with intratubular nonpolarizable calcium phosphate crystals. *(ABF/Vanderbilt Collection.)*

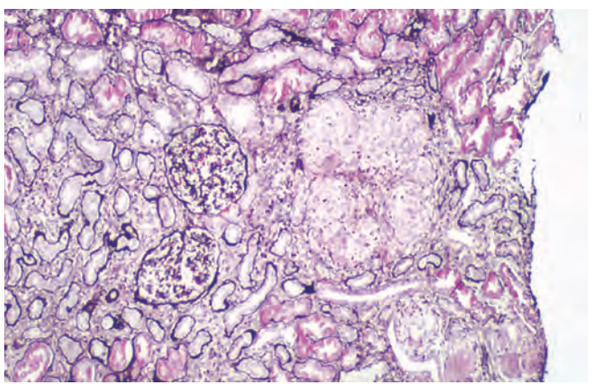

Figure e14-30 **Sarcoidosis.** There is chronic interstitial nephritis with numerous, confluent, non-necrotizing granulomas. The glomeruli are unremarkable, but there is moderate tubular atrophy and interstitial fibrosis. *(ABF/Vanderbilt Collection.)*

Figure e14-31 **Hyaline cast.** *(ABF/Vanderbilt Collection.)*

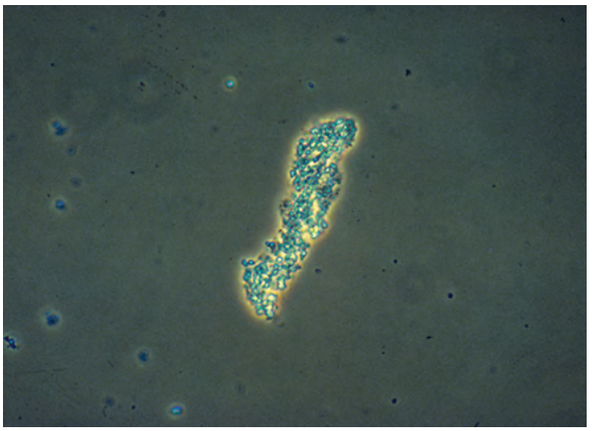

Figure e14-32 **Coarse granular cast.** *(ABF/Vanderbilt Collection.)*

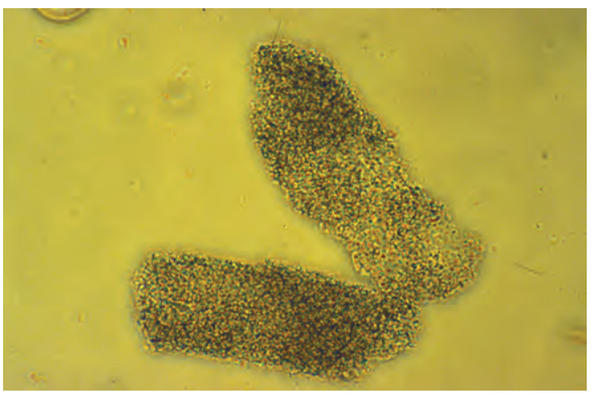

Figure e14-33 **Fine granular casts.** *(ABF/Vanderbilt Collection.)*

Figure e14-34 **Red blood cell cast.** *(ABF/Vanderbilt Collection.)*

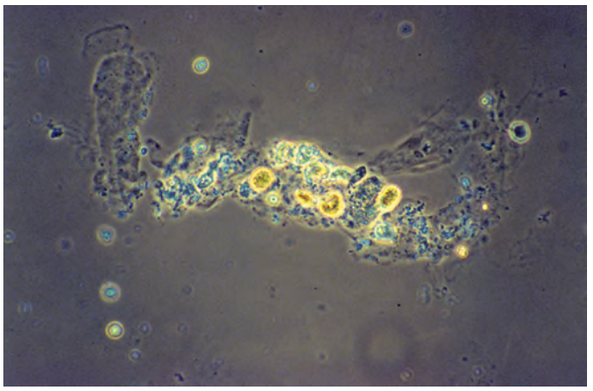

Figure e14-35 WBC cast. *(ABF/Vanderbilt Collection.)*

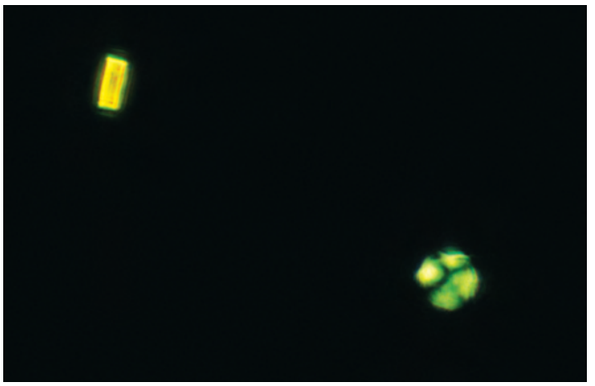

Figure e14-37 "Maltese cross" formation in an oval fat body. *(ABF/Vanderbilt Collection.)*

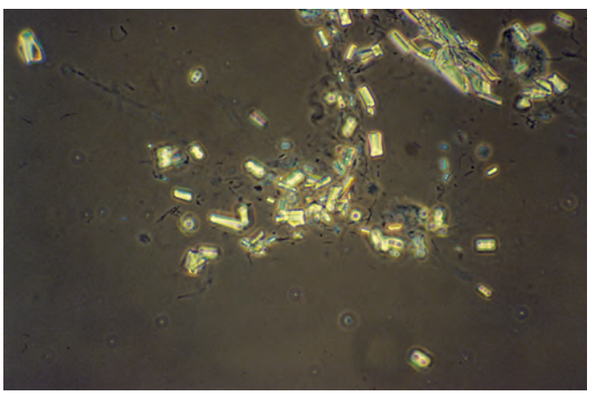

Figure e14-36 Triple phosphate crystals. *(ABF/Vanderbilt Collection.)*

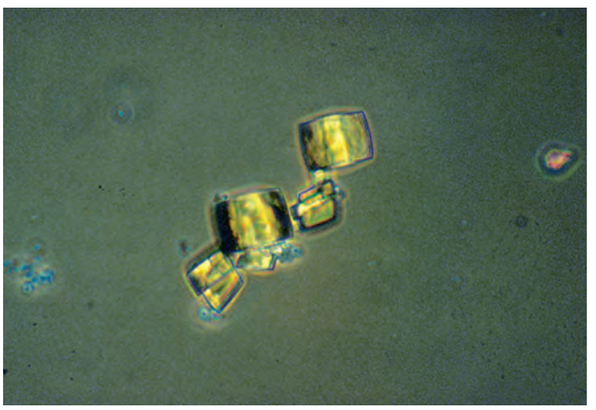

Figure e14-38 Uric acid crystals. *(ABF/Vanderbilt Collection.)*